13th UK Heat Transfer Conference, UKHTC2013
2 - 3 September 2013
Imperial College London

Design and Analysis of a Thermally Driven Thermoacoustic Air Conditioner for Low Grade Heat Recovery

Zhibin YU

School of Engineering, University of Glasgow, Glasgow, Scotland, United Kingdom
Email: Zhibin.Yu@glasgow.ac.uk

Abstract

This paper presents the design and analysis of a thermally driven thermoacoustic cooler, which aims to utilise industrial waste heat to provide air-conditioning for buildings where waste heat are abundant but air conditioning is required. The working gas is helium at 3.0 MPa. The operating frequency is around 100 Hz. A three-stage travelling wave thermoacoustic engine is design to convert waste heat to acoustic power, and a single stage travelling wave thermoacoustic cooler is connected to the engine to provide cold water at temperature of 0-5 °C for air conditioning. The ambient temperature is set as 40 °C. The simulation results show that the engine can convert 9.9% of the 15 kW heat input (at a temperature of 200 °C) to 1.5 kW acoustic power, and that the cooler can delivery 2.6 kW cooling power at 0 °C with a coefficient of performance (COP) of 2.25.

Keywords: thermoacoustic engine; thermoacoustic cooler; air-conditioning; heat recovery

1 Introduction

Thermoacoustic technology deals with the conversion between thermal energy and acoustic power (i.e., p-v power). A travelling wave thermoacoustic engine/cooler is essentially the acoustic equivalent of a Stirling engine/cooler; however it has several particular advantages, such as simplicity, reliability, and scalability.

Ceperley [1] was first to realize that when a travelling sound wave propagates though the regenerator from the cold to the hot end, the heat transfer interaction between the gas and the solid material undergoes a Stirling-like thermodynamic cycle. Strictly speaking, the thermoacoustic core (a regenerator sandwiched by the hot and ambient heat exchangers) just works as a power amplifier. To complete this Stirling-like thermodynamic process, acoustic power has to be fed to the ambient end of the regenerator with a near travelling-wave phasing. Travelling wave thermoacoustic engine has attracted enormous research efforts. Yazaki et al. [2] were the first to demonstrate a practical travelling-wave thermoacoustic engine. However, this engine proved very low efficiency due to the large viscous losses resulting from high acoustic velocities in the regenerator and the resonator. Late, De Blok [3] demonstrated a travelling wave engine with a bypass feedback mechanism, and Backhaus and Swift [4] proposed a different type, in which thermoacoustic core is placed within a torus with a length much shorter than the acoustic wavelength at the operating frequency. A long standing wave resonator is connected to this torus just after the secondary ambient heat exchanger. The thermal efficiency of the latter is 30%, equivalent to 41% of the theoretical Carnot efficiency. The recent progress on this type of travelling wave thermoacoustic engine has achieved 49% of Carnot efficiency [5].

Similar to Stirling engine, thermoacoustic engine can be externally heated with a variety of heat sources and are capable of utilising low grade waste heat. For such applications, the key challenge is to reduce the onset temperature difference of thermoacoustic engines, which is the minimal

temperature difference between the two ends of the regenerator to start the spontaneous acoustic oscillations. Different engine configurations have been developed to meet this challenge. De Blok designed a hybrid configuration with a travelling wave feedback waveguide, and successfully reduced the onset temperature difference to 65 K [6]. He recently also developed four-stage self-matching travelling wave thermoacoustic engine that can operate at a temperature difference as low as 40 K at each stage [7, 8]. This shows that thermoacoustic engines have the potential for utilising waste heat sources.

The acoustic power generated from thermal energy by the thermoacoustic engine can be used to drive a thermoacoustic heat pump. In this way, a thermally driven thermoacoustic heat pump can be developed, which has no moving parts and thus requires little maintenance. As such a heat pump does not involve any phase change processes of working medium, it can be applied to a variety of temperature ranges, such as those for refrigerator [9, 10], domestic and industrial heat pump [11], cryogenic coolers [12], and air conditioner.

One motivation behind this research is that, waste heat (100-250 °C) is abundant in a variety of factories, while cooling (or air conditioning) is required especially in hot seasons. The above mentioned thermoacoustic heat pump can be potentially applied to recover energy from waste heat.

This paper will study the feasibility of the development of such air conditioner. A multistage thermoacoustic engine combined with a thermoacoustic cooler is studied numerically. The whole system will be modelled and optimised using DeltaEC software (Design Environment for Low-amplitude ThermoAcoustic Energy Conversion), which was developed by the researchers at Los Alamos National Laboratory for predicting the performance of thermoacoustic devices [13]. The simulation results will be discussed in detail and compared with some published experimental data.

2 Concept

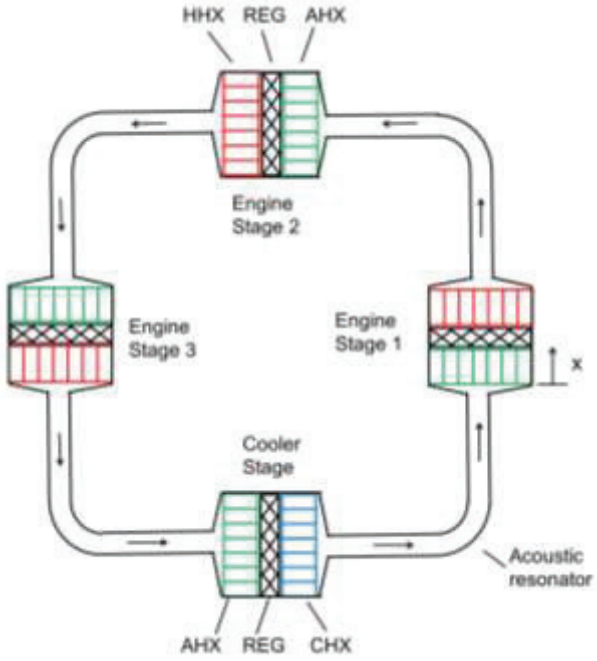

Figure 1: Schematic diagram of the waste heat powered thermoacoustic air conditioner

As mentioned in the introduction, the key challenge for utilising waste heat sources is the low operating temperature difference. Multi-stage travelling wave thermoacoustic engine is certainly the best solution as it has very low onset temperature differences. The system studied in this paper has the similar configuration and operating conditions as the thermoacoustic refrigerator developed by De Blok [8, 14], of which some experimental data was published. In this paper, the simulation results will

be compared with these data to validate our theoretical model which will be used to construct a thermoacoustic air conditioner prototype in the future.

Figure 1 shows the schematic diagram of this system. It has three engine units and one cooler unit. Each engine unit has a thermoacoustic core that has a regenerator (REG) sandwiched by an ambient heat exchanger (AHX) and hot heat exchanger (HHX). For the cooler section, the hot heat exchanger is replaced by a cold heat exchanger (CHX) to provide cooling load. The four thermoacoustic cores are connected with acoustic resonators that are ducts with a much smaller cross-sectional area than that of the thermoacoustic cores. The distance between the two neighbour units is about quarter wavelength.

The whole system starts the spontaneous acoustic oscillations when temperature at the hot heat exchangers reaches the onset conditions. The acoustic power flux will run through the loop. The acoustic power comes out from the cooler and feeds into the ambient end of the first engine unit, and then is amplified within its regenerator. In a similar way, the acoustic power is further amplified by the second and third engine stages. Finally, after some dissipation along the acoustic resonators, the acoustic power reaches the cooler. Part of the acoustic power is consumed by the cooler to pump heat from the cold end to the ambient end of regenerator. The remaining acoustic power runs into the first engine section to repeat the whole process.

3 Modelling

The whole system is modelled by using linear thermoacoustic theory [13, 15]. Steady-state sinusoidal oscillations of variables such as pressure, volumetric velocity, temperature, and density are written in the complex notation.

$$p = p_m + \mathrm{Re}\left[p_1(x)e^{i\omega t}\right], \tag{1}$$

$$U = \mathrm{Re}\left[U_1(x)e^{i\omega t}\right], \tag{2}$$

$$T = T_m + \mathrm{Re}\left[T_1(x)e^{i\omega t}\right], \tag{3}$$

and

$$\rho = \rho_m + \mathrm{Re}\left[\rho_1(x)e^{i\omega t}\right]. \tag{4}$$

In the above equations, p, U, T, ρ, and γ are the pressure, volumetric velocity, temperature, density and the ratio of specific heat capacities of the gas, respectively; ω and a are the angular frequency and sound speed of the acoustic wave; f_k and f_v are the spatially averaged thermal and viscous functions, respectively. Subscript "1" indicates the first order of a variable, which usually has a complex amplitude. Based on the above assumptions, equation (5) was derived to quantitatively describe the interaction between the acoustic and temperature fields (i.e. the thermoacoustic effect).

$$\left[1+(\gamma-1)f_k\right]p_1 + \frac{\gamma p_1}{\omega^2}\frac{d}{dx}\left(\frac{1-f_v}{\rho_m}\right) - \frac{a^2}{\omega^2}\frac{f_k-f_v}{1-\sigma}\frac{1}{T_m}\frac{dT_m}{dx}\frac{dp_1}{dx} = 0 \tag{5}$$

For the convenience of numerical calculations, equation (5) can be written as:

$$dp_1 = -\frac{i\omega\rho_m dx/A}{1-f_v}U_1, \tag{6}$$

$$dU_1 = -\frac{i\omega A dx}{\gamma p_m}\left[1+(\gamma-1)f_k\right]p_1 + \frac{(f_k - f_v)}{(1-f_v)(1-\sigma)}\frac{dT_m}{T_m}U_1. \tag{7}$$

Equations (6) and (7) are the thermoacoustic version of momentum and continuity equations. Based on the linear model, a computer package DeltaEC. It integrates equations (6) and (7) numerically, segment by segment, throughout the whole device based on the low amplitude acoustic approximation and sinusoidal time dependence [11].

4 Performances

For each stage, the engine efficiency is defined as the ratio of the net acoustic power W_a production over the heat input Q_{in} to the hot heat exchanger.

$$\eta_i = \frac{W_{a,i}}{Q_{in,i}}. \tag{8}$$

For the whole system, the overall engine efficiency is defined as

$$\eta_m = \frac{\sum_i W_{a,i}}{\sum_i Q_{in,i}}, \; i=1, 2, 3. \tag{9}$$

The coefficient of performance (*COP*) indicates the performance of a cooler and is defined as the ratio of the cooling load of the cooler Q_c over the acoustic power $W_{a,c}$ it consumes,

$$cop = \frac{Q_c}{W_{a,c}}. \tag{10}$$

The overall energy efficiency is defined as the ratio of the cooling power over the total heat input to the three engine stages.

$$\varepsilon = \frac{Q_c}{\sum_i Q_{in,i}}. \tag{11}$$

5 Simulation Results and discussion

The design philosophy of such a thermoacoustic device is to locate both engine and cooler units close to travelling wave region within the acoustic field to maximise the acoustic and cooling power production, and also to tune the phase within the acoustic resonator close to travelling wave condition to minimise the acoustic losses. To achieve this, the optimisation mainly focuses on the impedance matching between the thermoacoustic engine and cooler.

The operating frequency is set as 100 Hz. The working gas is helium with pressure of 30 bar. The heat source temperature is set as 200 °C, while the ambient temperature is set as 40 °C for some extreme weather conditions. The cooling for air-conditioning is usually in the range of 5-10 °C. In the simulation, the cooling load temperature is set as 0 °C.

The regenerators are selected as stainless mesh screens which has a porosity of 0.7 and hydraulic radius of 75 microns. All of the heat exchangers have a shell-and-tube configuration, of which the porosity, hydraulic radius and length are 0.4 and 1 mm and 4 cm, respectively. Four thermoacoustic cores have the same cross sectional area of 0.01 m^2. The acoustic resonator pipe has a much smaller cross section area of 0.0014 m^2. The pressure amplitude is about 7% of the mean pressure. As

indicated in Fig.1, the iteration starts from the ambient heat exchanger of the first engine stage. The total length of the loop is about 9.6 m. The main simulation results are summarized in Table 1.

Table 1: Summary of simulation results

Symbol	Definition	Unit	Engine 1	Engine 2	Engine 3	Cooler
T_h	Solid Temperature at HHX	°C	200	200	200	-
T_a	Solid Temperature at AHX	°C	40	40	40	40
T_c	Solid Temperature at CHX	°C	-	-	-	0
$W_{a,\,in}$	Acoustic power inlet	W	2304	2765	3016	3518
$W_{a,\,out}$	Acoustic power outlet	W	2843	3119	3644	2363
$W_{a,\,net}$	Net acoustic power production (engine) or consumption (cooler)	W	539	354	628	1156
$Q_{in,i}$	Heat input to HHX (engine) or CHX (cooler)	W	4167	6198	5026	2600
η_i	Efficiency for each stage	%	12.9	5.7	12.5	-
η_m	Average engine efficiency	%	9.9			-
COP	Coefficient of performance		-			2.25
η_{Carnot}	Carnot Efficiency: (Th-Ta)/Th	%	32.9			-
$COPC$	Carnot COP: Tc/(Ta-Tc)		-			6.8
η_r	Percentage of Carnot Efficiency	%	30			-
$COPR$	Percentage of Carnot COP	%	-			33

As shown in Table 1, the total heat input to three engine stages is about 15 kW. The total acoustic power production is about 1521 W. The overall thermal-to-acoustic efficiency is about 9.9%. The theoretical Carnot engine efficiency is about 32.9% for such heat source and sink temperature. Therefore, this system achieves about 30% of the ideal maximum efficiency. De blok recently reported that his small size four-stage travelling engine with similar configuration achieved 34% of the Carnot efficiency when the heat source temperature was 211 °C [14]. The simulation results obtained here agree with de blok's experiments very well although the power output level is much different.

The cooler stage consumes 1156 W acoustic power, and pumps 2600 W heat from 0 to 40 °C. The corresponding COP is about 2.25. This is equivalent to 33% of the ideal Carnot COP for this temperature range, which is about 6.8. De blok's refrigerator reached a temperature of -40.5°C, obtained COP was about 29% of the ideal Carnot COP. The simulation results of the cooler are also very close to de Blok's experimental results [14]. The overall energy efficiency is about 17.3%. The good agreement between this simulation and the published experimental results validates our model.

Table 1 also showed some interesting and unexpected phenomena. Although the three engine stages have exactly the same dimensions and configuration, the acoustic power production and thermodynamic efficiencies are different for each stage. The heat input is also quite different for the same temperature at hot heat exchange. These phenomena indicate that the system is not really acoustically symmetric to each engine section. To further understand what causes these differences, the acoustic fields along the loop needs to be studied in detail. The distribution of the amplitude of acoustic pressure, volumetric velocity, phase angle between pressure and velocity oscillation, impedance, and acoustic power flux have been extracted from the simulation results and shown in Figs. 2 – 6, respectively.

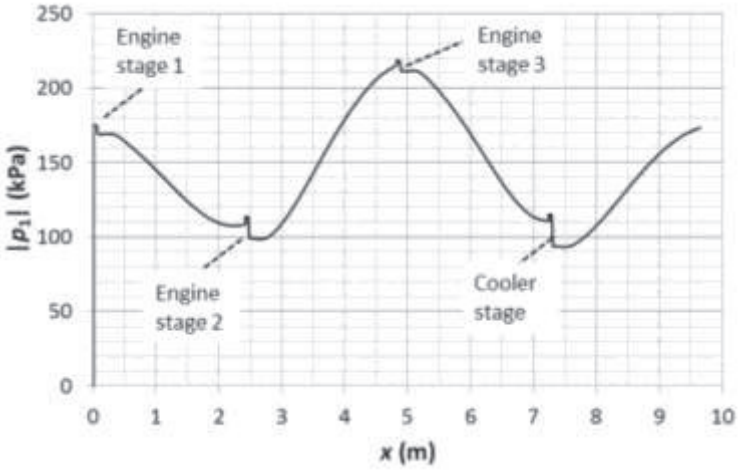

Figure 2: Distribution of the amplitude of acoustic pressure along the loop

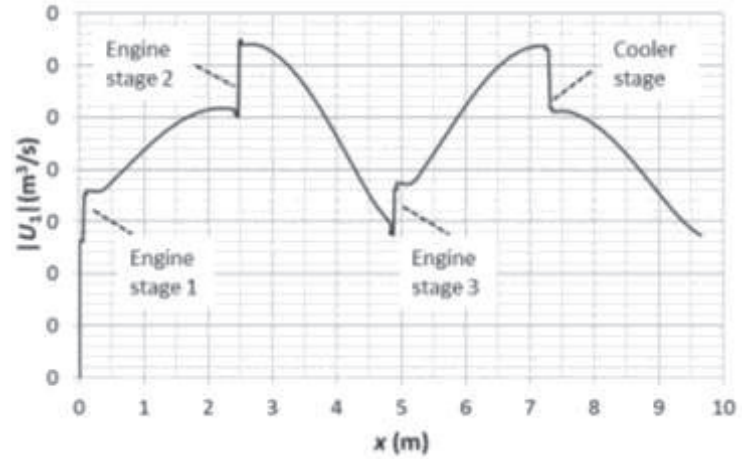

Figure 3: Distribution of the amplitude of volumetric velocity along the loop

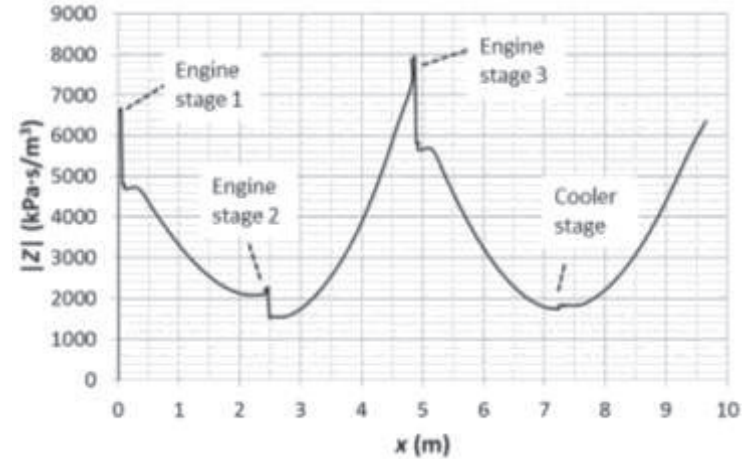

Figure 4: Distribution of the amplitude of acoustic impedance along the loop

Figure 2 shows the distribution of the amplitude of the acoustic pressure along the loop. It can be seen that there is maximum pressure amplitude about 220 kPa near engine stage 3, and there is minimum pressure amplitude 92 kPa near the cooler about. The standing wave ratio can be estimated by the ratio of these two pressure amplitudes as 2.39. This means that the acoustic reflection within the resonator is still relatively high. It can also be seen that both engine stages 1 and 3 locate at high pressure amplitude region, while the engine stage 2 and cooler locate at low pressure amplitude. The sharp drops of pressure amplitude appear at four regenerators where the flow resistance is very high.

Similarly, Fig. 3 shows the distribution of the amplitude of volumetric velocity along the loop. It can be seen that there are two peaks and two troughs along the loop. Engine units 1 and 3 locate close to these two peaks, while the engine stage 2 and cooler locate at the troughs. Due to the sharp temperature gradient along the regenerators, there is sharp increase of volumetric velocity at each regenerator of engine stages and a sharp decrease at the cooler regenerator.

To further this analysis, the acoustic impedance along the loop has been calculated as shown in Fig. 4. It can be found that the engine stages 1 and 3 locate at high impedance region, while the engine stage 1 and cooler stage locate at low impedance region. Low impedance usually means high acoustic velocity and high acoustic losses in the regenerator. This explains the low efficiency at engine stage 2.

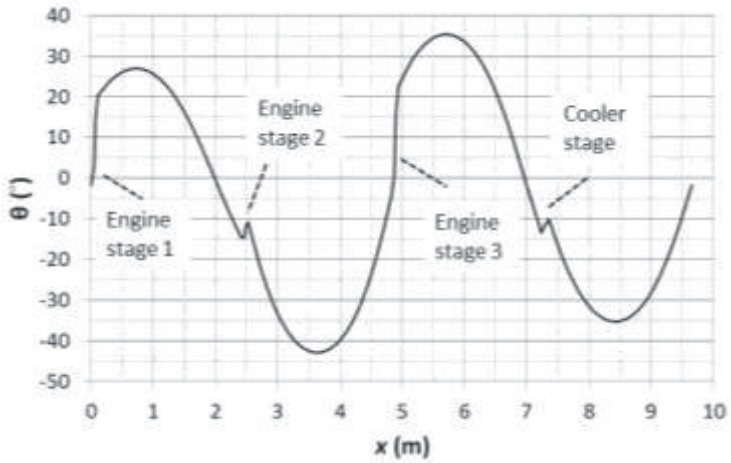

Figure 5: Phase angle θ between pressure and velocity oscillations along the loop

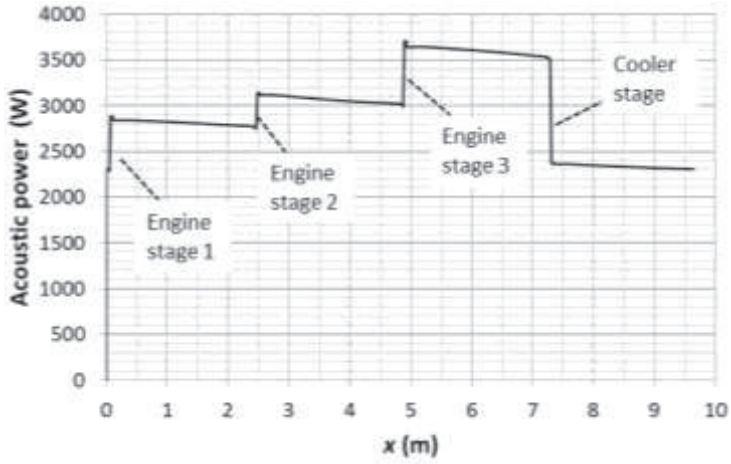

Figure 6: Distribution of the acoustic power flux along the loop

Figure 5 shows the phase difference between pressure and velocity oscillations along the loop. It can be found that all engine stages and the cooler are located in a travelling wave zone (i.e., θ is close to zero). Most of the resonator operates with a near travelling wave condition (i.e., $-30<\theta<30^{\circ}$). It should be noted that a small section of the resonator have a phase angle about - 42°, which indicates high local acoustic losses. Some phase tuning technique such as tuning stub may be introduced to tune the phase angle down to near zero [16]. Fig. 6 shows the acoustic power flux along the loop. It clearly shows the acoustic power is generated at each engine stage and dissipated along the resonator, heat exchanger, and the cooler.

6 Conclusion and Future Work.

This paper reports the numerical design and analysis of a thermoacoustic engine driven thermoacoustic cooler. It can be potentially applied to providing air-conditioning for places where the waste heat is abundant but the cooling is required. The simulation results have been compared with

published data, and showed a good agreement. The system can achieve a thermal-to-acoustic efficiency of 9.9% at the engine stages, and a COP of 2.25 at the cooler stage, which are about 30% of the ideal Carnot engine efficiency and COP. Some problems, e.g. the relative high standing wave ratio, have been identified. In the future, the model will be further optimised to achieve a better performance. A small scale prototype will be built and tested.

References

[1] Ceperley, P.H., A pistonless Stirling engine-the travelling wave heat engine, Journal of the Acoustical Society of America, vol 66, pp1508–1513, 1979.

[2] Yazaki, T., Iwata, A., Maekawa, T., and Tominaga, A. Traveling wave thermoacoustic engine in a looped tube. Phys. Rev. Lett. Vol 81, pp 3128–313, 1998.

[3] De Blok, K. "Thermoacoustic system," Dutch Patent. International Application Number PCT/NL98/00515 (1998)

[4] Backhaus, S. and Swift, G.W., A thermoacoustic-Stirling heat engine: Detailed study, Journal of Acoustical Society of America, vol 107(6), pp 3148-3166, 2000.

[5] Tijani, M. E. H. and Spoelstra, S. A high performance thermoacoustic engine. J. Appl. Phys. 110: 093519, 2011.

[6] De Blok, K. Low operating temperature integral thermoacoustic devices for solar cooling and waste heat recovery. Acoustics'08, Paris, June 29-July 4 2008.

[7] De Blok, K. Novel 4-stage traveling wave thermoacoustic power generator. FEDSM2010-ICNMM2010August 2-4, 2010, Montreal, Canada

[8] De Blok, K. Multi-stage traveling wave thermoacoustics in practice. The 19th International Congress of Sound and Vibration, Vilnius, Lithuania, July 8-12, 2012.

[9] Adeff, J.A. and Hofler, T.J., Design and construction of a solar thermal powered thermo-acoustically driven thermoacoustic refrigerator, Journal of Acoustical Society of America, vol 107(5), pp 2795, 2000.

[10] Dai, W., Luo, E., Zhang, Y. and Ling, H., Detailed study of a traveling wave thermoacoustic refrigerator driven by a thaveling wave thermoacoustic engine, Journal of Acoustical Society of America, 19(5), 2686-2692, 2006.

[11] Tijani, H., Spoelstra, S., and Lycklama J.A. high temperature thermoacoustic heat pump. The 19th International Congress of Sound and Vibration, Vilnius, Lithuania, July 8-12, 2012.

[12] Chen, Y.Y., Luo, E. and Dai, W. Heat transfer characteristics of oscillating flow regenerators in cryogenic temperature range below 20 K. Cryogenics 49(7), 313–319, 2009

[13] Ward, B., Clark, J. and Swift, G. W., Design Environment for Low-Amplitude ThermoAcoustic Energy Conversion (DELTAEC) program. USA, Los Alamos National Laboratory, New Mexico, 2008.

[14] http://www.aster-thermoacoustics.com/

[15] Swift, G. W., Thermoacoustics: a unifying perspective for some engines and refrigerators, Acoustical Society of America through the American Institute of Physics, 2002.

[16] Yu, Z., Jaworski, A.J., and Backhaus, S. Travelling-wave thermoacoustic electricity generator using an ultra-compliant alternator for utilization of low-grade thermal energy. Applied Energy, Vol 99, pp135-145, 2012